Agricultural Water Management 216 (2019) 138–152

Contents lists available at ScienceDirect

Agricultural Water Management

journal homepage: www.elsevier.com/locate/agwat

Modeling climate-smart decision support system (CSDSS) for analyzing water demand of a large-scale rice irrigation scheme

M.K. Rowshon[a,*], N.S. Dlamini[a], M.A. Mojid[b], M.N.M. Adib[a], M.S.M. Amin[c], S.H. Lai[d]

[a] Department of Biological and Agricultural Engineering, Universiti Putra Malaysia, 43400 UPM Serdang, Selangor, Malaysia
[b] Department of Irrigation and Water Management, Faculty of Agricultural Engineering and Technology, Bangladesh Agricultural University, Mymensingh, 2202, Bangladesh
[c] Faculty of Sustainable Agriculture, Universiti Malaysia Sabah (UMS), Malaysia
[d] Department of Civil Engineering, Faculty of Engineering, University of Malaya, 50603 Kuala Lumpur, Malaysia

ARTICLE INFO

Keywords:
Rice cultivation
Irrigation water demand
Climate change
Global climate models
Climate-smart DSS

ABSTRACT

Climate projection at local scale is one of the crucial challenges that affects the development of water management-related mitigation plans. Moreover, the currently available climate models do not directly simulate some of the hydro-climatic parameters (e.g., effective rainfall, reference evapotranspiration, irrigation requirements), which are of interest in irrigation sector. Modeling crop-water demands under changing climate involves several step-by-step approaches that are tedious and time-consuming for many water users. This study developed a water management tool, hereafter called Climate-Smart Decision-Support System (CSDSS), for modeling water demand of rice irrigation schemes under climate change impacts. The CSDSS is a user-friendly interactive program consisting of three main modules integrated in MATLAB and a graphical user interface development environment (GUIDE). The model runs with ten Global Climate Models (GCMs) and three emission scenarios (RCP 4.5, 6.0 and 8.5). It can generate several hydro-climatic parameters based on a daily water balance model, with input data from GCMs projections, crop, soil and field conditions. The model allows water managers to make fast decision for paddy water management. The generated outputs can be obtained through individual GCMs as well as through multi-models (ensemble) projection and can be converted into excel format for further analysis. The model was applied to evaluate the impacts of climate change on irrigation water demand and other key hydro-climatic parameters in Tanjung Karang Rice Irrigation Scheme in Malaysia for the period 2010–2099 with reference to the baseline period of 1976–2005. The results show that irrigation water demand will increase during the off-season (January–June) but decrease during the main season (July–December) due to significant contribution from effective rainfall in the latter season. The CSDSS tool can be used for managing water resources under changing climate and would, therefore, be helpful in promoting appropriate adaptation and mitigation strategies that can lead to more sustainable water use at farm level. Some future improvements of the tool, due to methodological limitations of the study, will however improve its performance.

1. Introduction

Inter-governmental Panel on Climate Change (International Panel for Climate Change (IPCC, 2007) identified three main signals of climate change: gradual increase in global average temperatures, rise in mean sea levels, and changes in rainfall patterns across the globe. It is thought that climate change will take the world into a new phase of water stress and uncertainty in the future. Many studies reveal that climate change will lead to a sharp increase in water demand by altering the hydrological cycle and affecting agricultural water supplies (Jang et al., 2007; Kirby et al., 2015; Mojid et al., 2015; Kirby et al., 2016; Wang et al., 2014). Increase in temperature and change in rainfall patterns will lead to higher crop evapotranspiration (water demand) and water shortage in stream flows (water availability). The impacts of climate change influence irrigation requirements (Schlenker et al., 2007) and are particularly sensitive to changes in precipitation and temperature (Frederick and Major, 1997). Previous studies showed that even small changes in rainfall intensity can result in significant impacts on stream flow (Risbey and Entekhabi, 1996). Acharjee et al. (2017) investigated the impacts of climate change on future water

* Corresponding author.
E-mail addresses: rowshon@yahoo.com, rowshon@upm.edu.my (M.K. Rowshon).

https://doi.org/10.1016/j.agwat.2019.01.002
Received 3 September 2018; Received in revised form 25 December 2018; Accepted 5 January 2019
Available online 13 February 2019
0378-3774/ © 2019 Elsevier B.V. All rights reserved.

requirements for long-term water resources management and agricultural planning. They emphasized on close monitoring and periodic evaluations to understand future directions of change in rainfall amounts and distribution. Ye et al. (2015) explored the temporal and spatial influence of climate change on suitable rice-cropping areas, rice-cropping systems and crop-water requirements during the growing season for historical (1951–2010) and future (2011–2100) time periods in China. Their study aimed to provide a scientific guideline for planning future cropping systems and optimizing water management. In addition to the water requirements, climate change affects several other aspects of rice cultivation systems, such as cultivated land and length of crop-growing season (Yoo et al., 2012, 2013).

Rice is the most common staple food for majority of the world's population, with more than 142 million hectares area under cultivation. Ninety percent of this area is in the monsoon regions of Asia (De Wrachien, 2003; FAO, 2013), of which 75% is under irrigation and the remaining is rainfed. Global rice consumption is projected to increase by 35% in 2020 relative to the 1995 baseline (Lee et al., 2005). It is envisaged that climate change will put a severe strain on future water resources for food, especially rice, production under irrigation. Therefore, the contradictory occurrences of increasing food demand and decreasing water availability warrant development of smart water management tools that would be consistent with future water resources planning and management under climate forcing.

In general, assessments of climate change require future climate scenarios, which can be derived either from the past climatic data with statistical approaches, synthetic climate scenarios, or outputs of global circulation models (GCMs). Assessment studies using GCM-outputs are widely becoming a basis of understanding the implications of climate change impacts in the context of future irrigation water demands both at global and scheme levels. The GCMs are incredible tools to study the impact of climate change and have been used globally in a number of recent studies. Wilby and Harris (2006) obtained most credible results by using GCM approach compared to other approaches. However, direct use of GCMs is restricted due to coarse spatial resolution of their outputs. So, it is necessary to downscale the GCM outputs (atmospheric predictor variables) to local-scale surface variables (Wilby et al., 2002). Several statistical downscaling approaches and models, such as delta change factor methodology, WXGEN model (Sharpley, 1990), CLIGEN model (Nicks et al., 1995), SDSM (Wilby et al., 2002), LARS-WG (Semenov et al., 2002), ClimGen (McKague et al., 2003) and EARWIG (Kilsby et al., 2007) have been developed in recent years. A number of global studies (e.g., Doll, 2002; Fischer et al., 2007; Elgaali et al., 2007; Yano et al., 2007; Diaz et al., 2007; de Silva et al., 2007; Knox et al., 2010; Shahid, 2011; Wang et al., 2014) were also done to assess the impact of climate change on regional and local-scale irrigation water demand based on perturbed climate change scenarios generated with GCM outputs or by using models.

Despite a good number of available tools, the downscaling procedure is still tedious, complex and computationally problematic for many stakeholders like farmers and water managers who may be laymen in this field. Moreover, the GCMs do not simulate the hydro-climatic parameters of interest in irrigation practice, such as crop evapotranspiration and irrigation water demand. Further steps are required to obtain these parameters on a daily scale as required in practical irrigation. The main problem faced by irrigation managers in many large-scale rice schemes is estimating water demand under climate scenarios and supplying water at the head of distributaries of the canal network in advance. So, an easy-to-use decision-support system for rice irrigation management information system that can integrate climate-change impact assessment procedures (e.g., GCMs, RCPs scenarios, downscaling process, climate projections and baseline period) and interface for linking with water demand models can remove the difficulty. Such a tool can remove the task of downscaling; it simply requires the users to generate climate scenarios and import them into a water demand module for simulating water demand based on selected GCM-scenario combination. The objectives of this study was (i) to develop a MATLAB-based decision-support system, called Climate-Smart Decision-Support System for Rice Irrigation Management Information System (CSDSS-RIMIS), that can integrate climate-change impact assessment procedures (10 GCMs, three RCP scenarios of 4.5, 6.0 & 8.5, downscaling process, climate projections from 2010 to 2099 and climate baseline period of 1976 to 2005) and interface for linking with evapotranspiration models, and (ii) to apply and test the CSDSS-RIMIS tool in modeling irrigation water demand for a large-scale rice irrigation scheme under climate change impacts in Malaysia.

2. Methodological approach

Modeling crop-water demands under climate change scenario involves several tedious and time-consuming step-by-step approaches. First, the observed and GCM-projected daily hydro-meteorological data are needed for estimating reference evapotranspiration. Then, irrigation requirements of paddy fields and effective rainfall need to be estimated with a water balance model. Some other related data, such as crop coefficient, seepage-percolation rate, water application and conveyance losses, and irrigation command area are also necessary. The flowchart of the methodology adopted in this study is depicted in Fig. 1.

2.1. Study area

The command area of the Integrated Agricultural Development Area (IADA) was considered for developing CSDSS-RIMIS for modeling crop-water demand under climate change condition. The project, initially started as Tanjung Karang Rice Irrigation Project in 1936 and transformed to the IADA in 1978, is located in the district of Kuala Selangor and Sabak Bernam at 3.40 °N latitude and 100.59 °E longitude (Fig. 2). It covers an area of 19,030 ha, which is used for irrigated rice farming twice in a year: dry off season (January–June, called first season), and wet main season (July–December, called second season). The project area has an average rainfall of 1500 mm, mostly concentrated over October to January, with the highest rainfall in October and lowest in June. The average monthly air temperature, humidity, solar radiation and wind speed is 28 °C, 77%, 15.2–20.4 MJ $m^{-2}day^{-1}$ and 2.25 m s^{-1}, respectively based on data of Department of Irrigation and Drainage (DID) and Malaysian Meteorological Department (MMD). The average monthly meteorological data of the study area from 1990 to 2010 is presented in Table 1.

About one-half (51%) of the irrigation water requirement is supplied in the scheme by rainfall received as effective rainfall within the rice fields, and the rest comes from the Bernam River basin. For better management of irrigation water supply, the project area has been divided into four Irrigation Service Areas (ISAs) (ISA I, ISA II, ISA III and ISA IV), and irrigation is staggered by one month interval during planting. Water is diverted at the Bernam Headworks at maximum design discharge (30.6 m^3 s^{-1}) and conveyed through a 14.5-km feeder canal into the Tengi river. The water is then channeled by gravity flow

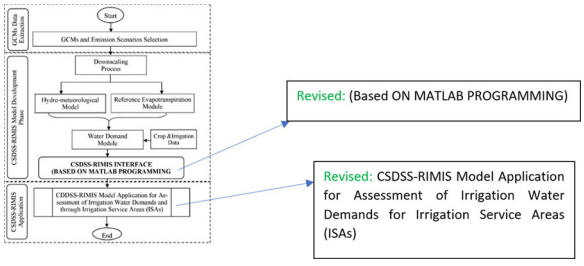
Start
GCMs and Emission Scenarios Selection
Downscaling Process
Hydro-meteorological Model
Reference Evapotranspiration Module
Water Demand Module
Crop &Irrigation Data
CSDSS-RIMIS INTERFACE (BASED ON MATLAB PROGRAMMING
CSDSS-RIMIS Model Application for Assessment of Irrigation Water Demands and through Irrigation Service Areas (ISAs)
End
Revised: (Based ON MATLAB PROGRAMMING)
Revised: CSDSS-RIMIS Model Application for Assessment of Irrigation Water Demands for Irrigation Service Areas (ISAs)

Fig. 1. Flowchart of methodology for development of Climate-Smart Decision-Support System for Rice Irrigation Management Information System (CSDSS-RIMIS) tool for modeling irrigation water demand under climate change scenarios.

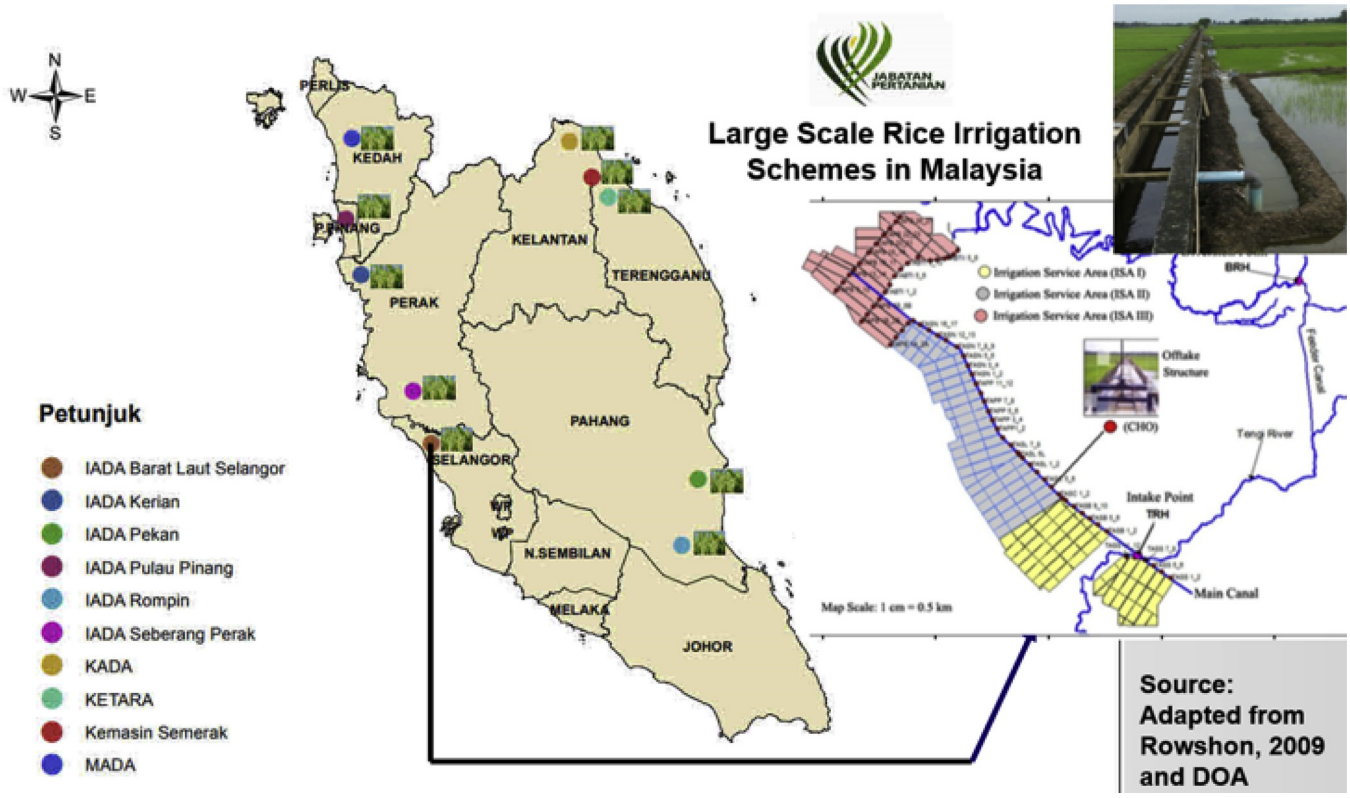

Fig. 2. Irrigation command area and structured irrigation networks in Tanjung Karang Rice Irrigation Scheme, Malaysia (Source: Rowshon et al., 2014, and JICA and DID, 1998).

Table 1
Average monthly hydro-meteorological data in the Integrated Agricultural Development Area (IADA) (Rowshon et al., 2014).

Month	Rainfall (mm)	T_{max} (°C)	T_{min} (°C)	Wind (km day^{-1})	Humidity (%)	Solar radiation MJ m^{-2} day^{-1}	ET_o (mm day^{-1})
January	119.4	30.8	23.2	77.8	79.0	17.3	3.9
February	108.7	31.3	23.5	86.4	78.1	19.8	3.7
March	109.9	31.7	24.1	90.7	78.9	20.4	4.1
April	131.9	32.0	24.5	88.1	80.6	20.0	3.9
May	102.1	32.4	24.6	86.4	80.1	19.3	4.1
June	71.7	32.5	24.2	88.1	78.7	19.1	4.1
July	114.9	32.0	23.9	94.2	78.5	18.7	4.2
August	96.8	31.7	24.0	95.0	78.7	18.0	4.1
September	148.6	31.1	24.0	91.6	80.1	17.3	3.8
October	198.3	30.9	23.9	94.2	81.6	16.9	3.9
November	194.2	30.7	23.7	82.1	82.9	15.4	3.7
December	145.2	30.6	23.4	76.0	81.5	15.2	3.8

to the intake point of the main canal and delivered to paddy fields through off-take structures consisting of constant head orifice structures.

2.2. Data and their sources

The observed climate data in the project area is of poor quality due to missing values for a series of years. So, a gridded daily hydro-meteorological dataset, developed by Wong et al. (2011) covering the whole Peninsular Malaysia, was used in this study, except the rainfall. The dataset included daily maximum and minimum air temperatures, wind speed and mean relative humidity. The data were gridded from the daily observed data at a spatial resolution of 5 km based on Angular Distance Weighting (ADW) procedure, which performed well in areas with sparse data as in Malaysia. The gridded data were developed using observed data obtained from different sources, including datalogger and telemetry network database of DID and MMD, Global Summary of the Day (GSOD) archive, Global Energy and Water Balance Experiment (GEWEX) research program, and Asian Monsoon Experiment (GAME) archive. Detailed overview of data processing, quality control and methodology used in data development was elaborated by Wong et al. (2009) and Wong et al. (2011). Three existing stations were considered to represent the historical spatial climate (1976–2005) of the scheme area. A threshold value of 1.0 mm was applied to remove small rainfall events following Deni et al. (2010) and Zin et al. (2010). The programming was developed following the irrigation scheme's current cropping calendar and irrigation distribution for the two seasons (off

Table 2
Current cropping calendar and distribution of irrigation supplies for the off and main irrigation seasons in Tanjung Karang Rice Irrigation Scheme.

Cropping activities	Off season				Main season			
	ISA I	ISA II	ISA III	ISA IV	ISA I	ISA II	ISA III	ISA IV
Pre-saturation	1-Jan	1-Feb	1-Mar	1-Apr	1-Jul	1-Aug	1-Sep	1-Oct
Sowing starts	15-Jan	15-Feb	15-Mar	15-Apr	15-Jul	15-Aug	15-Sep	15-Oct
Normal irrigation	1-Feb	1-Mar	1-Apr	1-May	1-Aug	1-Sep	1-Oct	1-Nov
Irrigation ends	10-Apr	10-May	10-Jun	10-Jul	10-Oct	10-Nov	10-Dec	10-Jan

Table 3
List of climate models used in the development of Climate-Smart Decision Support System, CSDSS.

Organization	GCM	Grid resolution	
		latitude	longitude
Canadian Centre for Climate Modeling and Analysis	CanESM2	2.80	2.80
National Center for Atmospheric Research	CCSM4	1.25	0.94
National Centre for Meteorological Research	CNRM-CM5	1.40	1.40
Centre for Australian Weather and Climate Research	CSIRO	1.80	1.80
NOAA Geophysical Fluid Dynamics Laboratory	GFDL-ESM2G	2.50	2.00
NOAA Geophysical Fluid Dynamics Laboratory	GFDL-ESM2M	2.50	2.00
Met Office Hadley Centre	HadGEM2-CC	1.88	1.25
Met Office Hadley Centre	HadGEM2-ES	1.88	1.25
Max Planck Institute for Meteorology	MPI-ESM-LR	1.88	1.87
Meteorological Research Institute	MRI-CGCM3	1.10	1.10

season and main season) as given in Table 2.

2.3. Hydro-meteorological downscaling module

2.3.1. Climate data extraction and processing

Rainfall and evapotranspiration are the major hydro-meteorological variables that influence crop-water requirement (Knox et al., 2010; Diaz et al., 2007). Evapotranspiration is dominantly influenced by air temperature, wind speed, relative humidity and solar radiation. These hydro-meteorological data sets were obtained from ten GCMs from Coupled Model Inter-comparison Project Phase 5 (CMIPP5) under three emission scenarios of RCP4.5, RCP6.0 and RCP8.5. Some impact assessment studies on water demand used the Special Report on Emission Scenarios (SRES) (Rehana and Mujumdar, 2012; Chung and Nkomozepi, 2012; Shahid, 2011). However, we used the latest scenarios, called Representative Concentration Pathways (RCPs), which are a new set of greenhouse gas scenarios represented by RCPs 2.6, 4.5, 6.0 and 8.5. Table 3 lists the GCM models used in the development of Climate-Smart Decision Support System, CSDSS. GCMs grid points were selected on the basis of stations' locations within the scheme area in terms of their longitude and latitude. Each GCM had four grid points, and a representative grid point was chosen based on the average value where the values were computed on all grid points and averaged to a single weighted value. The data was prepared in three future periods of 30-year time segments centered on 2020s (2010–2039), 2050s (2040–2069) and 2080s (2070–2099).

2.3.2. Hydro-meteorological downscaling

Because of coarse resolution of GCMs' projections, their outputs cannot be utilized directly in water demand modeling. So, the GCMs' output was downscaled to bridge the gap. The downscaling task is, however, complex and time-consuming for assessing the risk of climate change impacts and selecting adaptation strategies. In this study, a hydro-meteorological graphical user interface was developed that integrates the common procedures of assessing climate change impacts integrated with GCMs and scenarios selection, and downscaling procedures of climate variables and their future projections. The interface also links the water-demand model in the computational steps. The interface is based on methodology of delta change factor as a statistical downscaling algorithm to create high resolution future variables at the station scale. Delta change is the most commonly adopted statistical downscaling technique used as an ordinary bias correction method to reduce bias between the observed station data and GCMs' outputs (Chen et al., 2011; Ouyang et al., 2015). The algorithm modifies the observed daily time series of the climate variables by adding and/or multiplying monthly mean changes of GCM outputs using adjusting formulas. The adjusting formulas for modified daily rainfall are expressed by Eqs. (1) and (2), and the modified daily series of temperature and other parameters are expressed by Eqs. (3) and (4). Due to lack of good quality data in the study area before stating of the project in 1976, a baseline period of 1976–2005 was adopted in this study.

$$RF_{delta} = (\overline{RF}_{future}/\overline{RF}_{control})_{monthly} \quad (1)$$

$$RF_{future,\,daily} = RF_{observed,daily} \times RF_{delta} \quad (2)$$

$$T_{delta} = (\overline{T}_{future} - \overline{T}_{control})_{monthly} \quad (3)$$

$$T_{future,\,daily} = T_{observed,daily} + T_{delta} \quad (4)$$

In the above equations, the notations RF and T imply rainfall and temperature, respectively. The subscripts 'delta, daily' denotes the downscaled daily variable using the delta method; 'observed, daily' denotes daily observations; 'future' denotes the average monthly GCM output for the future period; and 'control' denotes the average monthly GCM output for the control or baseline period. The module was developed using MATLAB graphical user interface containing several scripted functions, including data extraction, processing and downscaling functions. The step-by-step procedures, followed in simulating the climate sequences in the hydro-meteorological interface, are illustrated in Fig. 3. The change factors for the GCM grid-box encompassing the command area are calculated for each month in the future years relative to the baseline. The interface can be applied to other geographical areas by simply incorporating the observed data of those stations and their corresponding baseline and future GCMs' outputs in the working folder. Additionally, the change factors can always be updated quickly if new GCMs and emission scenarios become available in the future. The change-factor technique has been widely applied in crop-water demand calculation and hydrological studies around the world (Chung and Nkomozepi, 2012; Knox et al., 2010; Diaz-Nieto and Wilby, 2005).

2.4. Reference evapotranspiration simulation module

Modeling irrigation water demand for assessing impacts of climate change requires estimating reference evapotranspiration (ET_o) for baseline period and future projections. The FAO Penman-Monteith model is widely adopted for estimating ET_o to provide relatively consistent values with actual crop-water use data worldwide (Allen et al., 1998). The model is expressed by

$$ETo_{t,s} = \frac{0.408\Delta(R_n - G) + \gamma\frac{900}{T+273}u_2(e_s - e_a)}{\Delta + \gamma(1 + 0.34u_2)} \quad (5)$$

where $ET_{ot,s}$ is standardized reference crop evapotranspiration for short grass (mm day^{-1}) in period t at downscaling station s, R_n is net radiation at the crop surface (MJ m^{-2} day^{-1}), G is soil heat flux density (MJ m^{-2} day^{-1}), T is air temperature at 2 m height (°C), u_2 is wind speed at 2 m height (m s^{-1}), (e_s–e_a) is saturation vapour pressure deficit (kPa), Δ is slope of vapour pressure curve (k Pa $°C^{-1}$), and γ is psychrometric constant (k Pa $°C^{-1}$). The downscaled hydro-meteorological variables, such as air temperature, relative humidity and wind speed were used as input to the ET_o model (Eq. (5)) for evaluating the anticipated changes. It is noted that solar radiation could not be downscaled directly owing to the non-existence of solar radiation data from GCMs archives. A simple temperature-based equation by Hargreaves and Samani (1982) was used to estimate the solar radiation (R_s) as

$$R_s = k_{rs}\,(T_{max} - T_{min})^{1/2} R_a \quad (6)$$

where k_{rs} is an adjustment factor that is equal to 0.16 for interior locations and 0.19 for coastal locations, T_{max} and T_{min} are the mean monthly maximum and minimum air temperatures (°C), respectively,

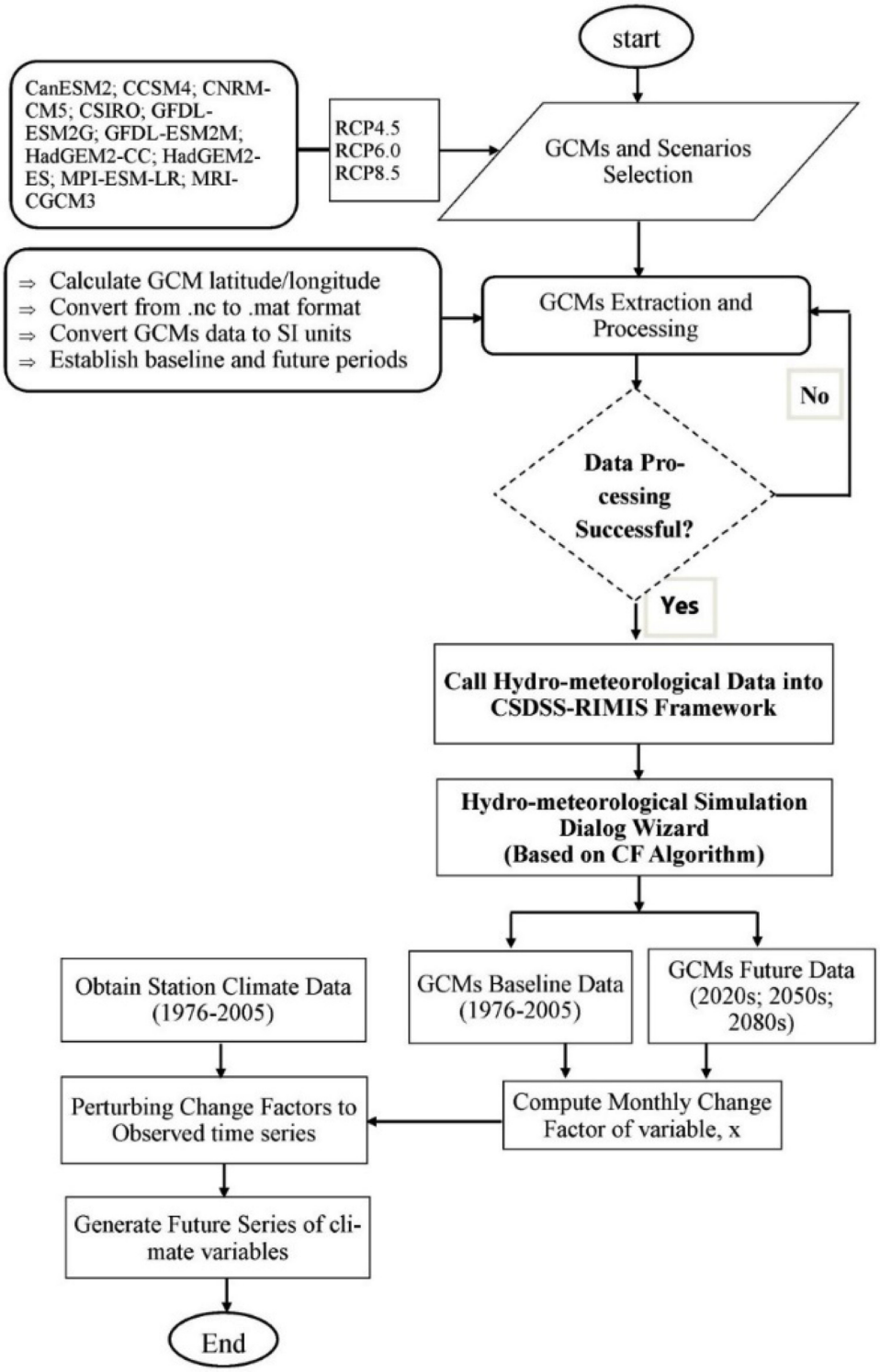
start
CanESM2; CCSM4; CNRM-CM5; CSIRO; GFDL-ESM2G; GFDL-ESM2M; HadGEM2-CC; HadGEM2-ES; MPI-ESM-LR; MRI-CGCM3
RCP4.5
RCP6.0
RCP8.5
GCMs and Scenarios Selection
⇒ Calculate GCM latitude/longitude
⇒ Convert from .nc to .mat format
⇒ Convert GCMs data to SI units
⇒ Establish baseline and future periods
GCMs Extraction and Processing
No
Data Pro-cessing Successful?
Yes
Call Hydro-meteorological Data into CSDSS-RIMIS Framework
Hydro-meteorological Simulation Dialog Wizard (Based on CF Algorithm)
Obtain Station Climate Data (1976-2005)
GCMs Baseline Data (1976-2005)
GCMs Future Data (2020s; 2050s; 2080s)
Perturbing Change Factors to Observed time series
Compute Monthly Change Factor of variable, x
Generate Future Series of cli-mate variables
End

Fig. 3. Schematic flowchart for hydro-meteorological simulation under climate forcing.

and R_a is extraterrestrial radiation (W m^{-2}), which was computed following Allen et al. (1998). A stand-alone graphical user interface was designed with several scripted codes and functions for the ET_o-module using MATLAB programming following a step-by-step process as illustrated in Fig. 4.

2.5. Crop-water demand simulation

2.5.1. Water balance model for rice fields

For evaluating the impact of climate change on irrigation water demand of rice, this study employed a daily time-step water balance model for rice field. The model utilized the concept of standing water depth (SW) as expressed by

$$SW_j = SW_{j-1} + IR_{j-1} + ER_{j-1} + ET_{j-1} + SP_{j-1} - DR_{j-1} \quad (7)$$

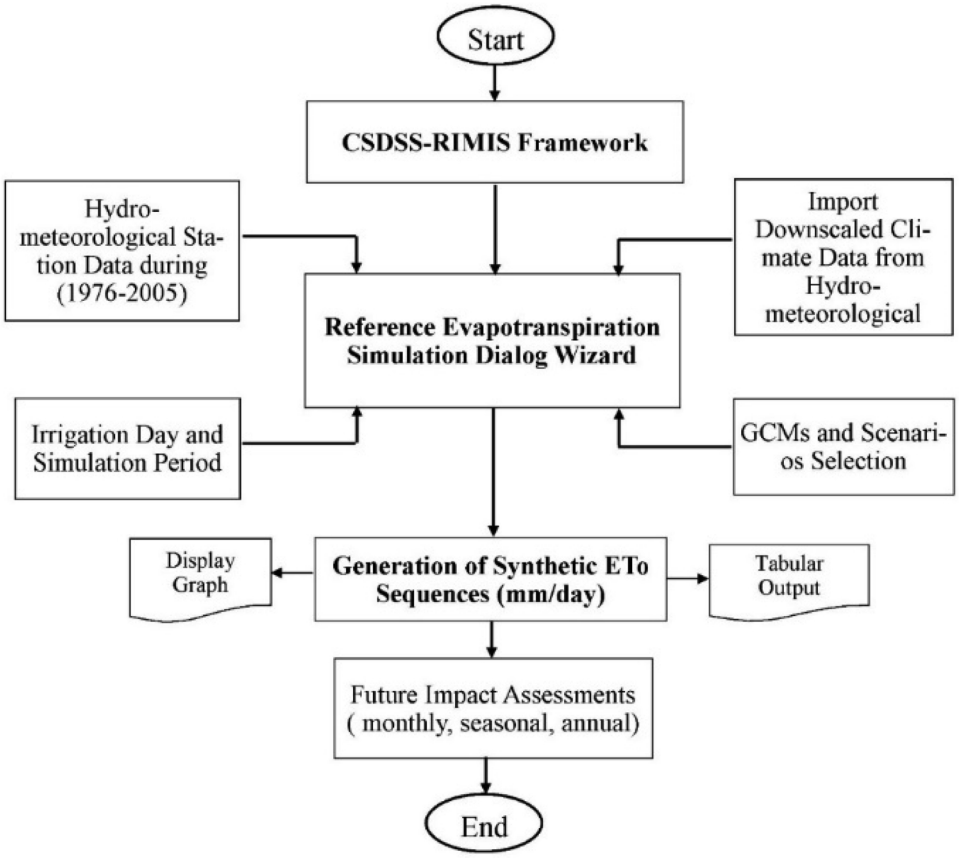

Fig. 4. Schematic flowchart for simulation of daily reference evapotranspiration (ET_o) sequences under climate change scenarios.

where SWj is water depth in the field on j-th day, SW_{j-1} is water depth in the field on (j-1)-th day, IR_{j-1} is the amount of applied irrigation on (j-1)-th day, ER_{j-1} is effective rainfall reaching the rice field on (j-1)-th day, ET $j-_1$ is crop evapotranspiration on (j-1)-th day, SP $j-_1$ is seepage and percolation losses from the rice field on (j-1)-th day, DR $j-_1$ is water lost through surface drainage on (j-1)-th day, and j is irrigation period. Different growth stages of rice with different maximum and minimum standing water depths – SW_{max} and SW_{min}, respectively, were allocated in the rice fields (Rowshon et al., 2014).

2.5.2. Effective rainfall

Effective rainfall is the portion of rain falling over the command area contributes to the water requirements of growing rice. The effective rainfall, ER_j (Eq. (7)), on period j at downscaling station s was estimated by using the drainage model of the International Rice Research Institute (IRRI, 1977) as

$$ER_{j,s} = RF_{j,s} \text{ for } DR_j = 0 \quad (8)$$

$$ER_{j,s} = RF_{j,s} - DR_j \text{ for } DR_j > 0 \quad (9)$$

where $RF_{j,s}$ is total rainfall on *j*-th day, $ER_{j,s}$ is effective rainfall on *j*-th day and DR_j is water lost through surface drainage on *j*-th day.

2.5.3. Crop evapotranspiration

Crop evapotranspiration (ET_c) was calculated based on relationship between reference evapotranspiration, ET_o, and crop coefficient (Eq. (10)) as

$$ETc_{j,p,s} = ETo_{j,p,s} \times Kc_{j,p,s} \quad (10)$$

where $ET_{c,j,p,s}$ is crop evapotranspiration (mm day^{-1}), $K_{cj,p,s}$ is crop coefficient (dimensionless), and $ET_{oj,p,s}$ is reference evapotranspiration (mm day^{-1}) of rice crop p for period j at downscaling station s. The crop coefficient values, experimentally determined by Chan and Cheong (2001) in several rice fields of the Tanjung Karang Irrigation Scheme, are depicted in Fig. 6. Reference evapotranspiration values were computed by using FAO Penman-Monteith method (Eq. (5)) from the reference evapotranspiration module based on GCMs data and imported to the water-demand simulation module.

2.5.4. Pre-saturation water requirements and seepage rate

MR84 is a widely adopted rice variety in Malaysia, with growth duration of 120–125 days. Wet direct seeding method is practiced in the irrigation scheme. Pre-saturation is an important initial stage prior to planting of rice crop. Water for pre-saturation was supplied at a rate of 18.5 mm day^{-1} ha^{-1} for a period of 14 days to the irrigation blocks of irrigation service area, ISA I (Table 2), followed by land preparation and drainage of excess water, if there was any. Similar supply rate was followed to irrigation blocks of the other irrigation service areas (ISAs II, III and IV), each staggered by one month form the other. The seepage and percolation rate were estimated as 1–3 mm day^{-1} following field test of DID and feasibility study of JICA (1998). Water requirements for pre-saturation in the water-demand simulation interface was determined by

$$P_{SAT}(k) = \frac{IR_{LS}(k) + EP_S(k) + SP(k) + SW(k)}{IE} \quad (11)$$

where P_{SAT} is water requirement (mm day^{-1}) during pre-saturation, $IR_{LS}(k)$ is water requirement (mm day^{-1}) to saturate the soil, $EP_s(k)$ is evaporation loss (mm day^{-1}) from saturated soil surface, SP(k) is seepage and percolation loss (mm day^{-1}), SW(k) is additional water supply (mm day^{-1}) to maintain the initial depth of flooding, IE is overall irrigation efficiency (fraction) and k is irrigation service area (ISA) number. IE varied from 50 to 65% depending on scheme management practices.

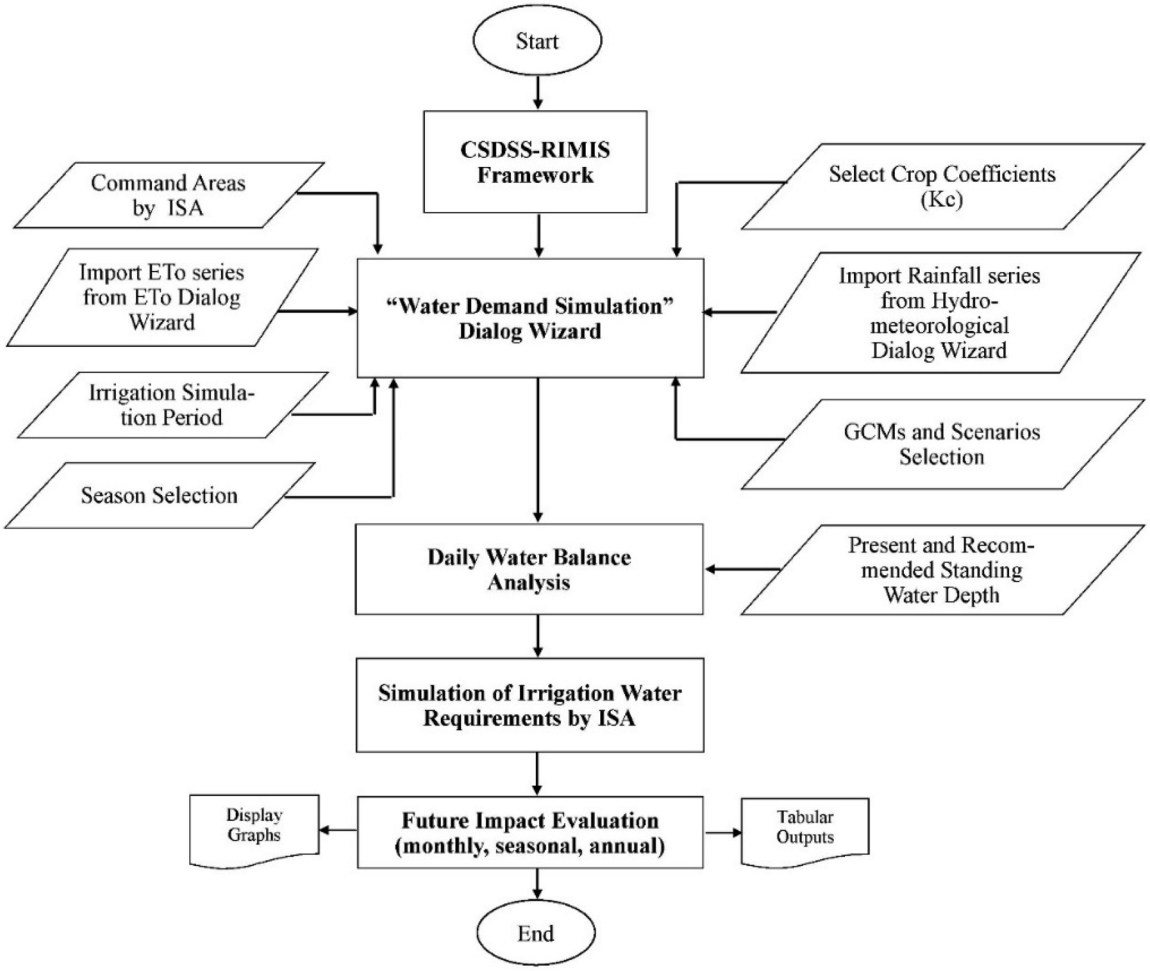

Fig. 5. Schematic flowchart for simulation of irrigation water demands under climate change scenarios.

2.5.5. Irrigation water requirement

Irrigation water requirement is the main consideration for planning, designing and day-to-day operation of an irrigation scheme. The irrigation water requirement, IRj, for k-th ISA on *j*-th day during normal irrigation period was estimated by

$$IR_j(k) = ET_j(k) + SP_j(k) - ER_j(k) + RP_j(k) - SW_{j-1}(k) \quad (12)$$

where RP is required ponding water depth during j-th day. The simulation process of irrigation water demand under climate change scenarios is illustrated in the working flow diagram of Fig. 5.

2.6. Design and development of DSS user-interface

The CSDSS-RIMIS tool consists of three basic modules: (i) hydro-meteorological simulation, (ii) reference evapotranspiration simulation, and (iii) water demand simulation; all modules are contained within a single working folder. In designing the interface, a criterion for modular development was adopted so that analyses can be done separately where necessary. The interface is structured in MATLAB with its graphical user-interface development environment (GUIDE), which is a useful platform to design user interface. The key advantage for using MATLAB is its computational capability. The interface is based on a mouse-driven approach with pop-up windows, pull-down menus and button controls. In designing the interface, several scripted functions, based on ten GCMs, were developed, each running under three RCP scenarios: RCP4.5, RCP6.0 and RCP8.5. The design of the interface includes creating GCMs calendars to account for GCMs with all 365 days in a year for computing change factors. The modules are interconnected through the graphical user interface, which provides users with ability to access data and outputs from the system. The GCMs data are contained in MATLAB database, allowing for quick update of data as new climate scenarios and GCMs become available.

On activation of the CSDSS-RIMIS model, the main dialog window appears in MATLAB environment. After activating dialog windows of the three modules, a simulation dialog window allows for generating daily sequences of hydro-meteorological variables. To run a simulation for rainfall, the user has to select the station, variable of interest, GCM-RCP scenario combination and simulation period by using the drop-down buttons. The future hydro-climatic parameters of a station are produced by perturbing the station. The parameters are derived by using change factors from the mean projected changes, which are simulated from GCMs for the same variables. Simulation outputs can be obtained from each of the ten GCMs or through multi-models' projections based on selected RCP emission scenario. The outputs can be generated as daily time series and long-term monthly time scale, and can be viewed as tables and graphs. The outputs are then imported to water-demand module for simulation of irrigation water demands.

For running the reference evapotranspiration simulation, the basic information like station, GCM-scenario and irrigation date are selected by using drop-down buttons in "Reference ET Simulation" dialog window. The hydro-meteorological variables, generated from the GCMs outputs, and their change factors are the main inputs in computing the reference evapotranspiration, ET_o. The time series of ET_o is generated for the selected irrigation period by pressing "Simulation of ET_o Time Series" button. The simulated ET_o outputs include daily ET_o series, mean monthly ET_o, multi-scenario comparisons and multi-future

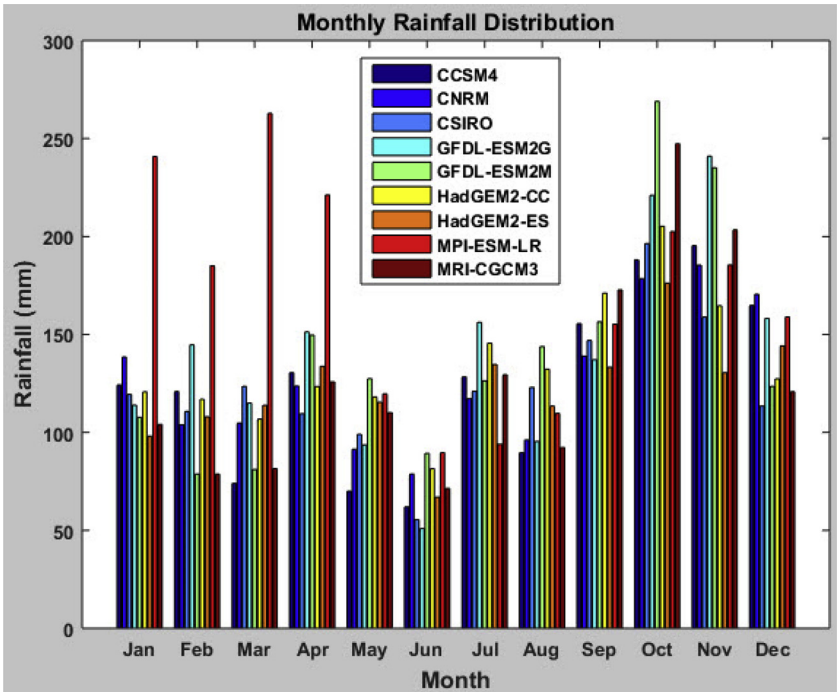

Fig. 6. Mean monthly rainfall outputs generated by GCM multi-models for 2050s period under RCP4.5 scenario.

comparisons. The ET_o outputs can be imported to the water-demand module for computing recommended irrigation water demands for the target irrigation areas.

The water-demand simulation module simulates irrigation demands by taking inputs from all irrigation service areas as the season advances. The user has to provide station, GCM-scenario and irrigation date in the simulation dialog window. The user also needs to adjust crop input data like length of growth stage, crop factors, irrigation efficiency, and seepage and pre-saturation rates. Daily ET_o and rainfall data are imported from the previous modules; effective rainfall is computed within the module. Other input data are provided by the model as default values that can be changed manually, if needed. With required input data, simulation of irrigation water demand is done by clicking the '*Simulate Future Scheme Water Demand*' button. The outputs can be viewed as tables and graphs. The module allows for saving the inputs and outputs into MATLAB database or in excel format.

The developed CSDSS tool was applied to Tanjung Karang Rice Irrigation Scheme to assess climate change impacts on key hydro-climatic parameters and irrigation water demands. Several outputs were generated from the model using both single GCM model(s) and multi-model projections. However, due to space constraint, only few selected outputs are discusssed in this paper.

3. Results and discussion

3.1. CSDSS-RIMIS model simulation outputs

3.1.1. Hydro-meteorological variables

Fig. 6 represents long-term monthly rainfall simulated by GCM models for 2050s period under RCP4.5 scenario. Most GCMs predicted higher annual rainfall compared to the baseline values, with the exception of CNRM, CSIRO and HadGEM2-ES models, which predicted 3.0%, 4.5% and 2.9% less rainfall compared to the baseline period. These differences in simulated monthly rainfall emphasize the uncertainties within the climate models in simulating rainfall.

Table 4 provides summary of analyses of changes in future rainfall on monthly time-scale for multi-scenario case for the periods 2010–2039, 2040–2069 and 2070–2099. Fig. 7 illustrates the projected mean monthly rainfall using multi-models and RCP scenarios for three future periods of 2010–2039, 2040–2069 and 2070–2099 relative to the baseline period of 1976–2005. RCP4.5 scenario shows increasing trends in monthly rainfall (also for future periods) except in June and December when the rainfall decreased by 3.7% (8%) and 2.9% (1.6%) in 2020s and 2080s, respectively. Under RCP8.5, the monthly rainfall distribution shows increasing trend in the near future (2020s) and a decreasing trend in January, February, March and December. However, RCP6.0 scenario shows a decreasing trend in all the months of the year and all future periods, with the greatest decrease in January (35.6%), February (26.4%) and March (32.6%). Climate projection in the study area, thus, reveals a decrease in rainfall in dry season (January–June) but increase in wet season (July–December).

Other rainfall-related outputs, such as effective rainfall, wet- and dry-spell lengths and weekly rainfall can also be generated from the interface. These analyses can be used periodically to compare the model outputs with station rainfall data for identifying climate change signals, its magnitude and direction of change. Such information can assist water managers and farmers in developing relevant adaptation and mitigation plans for irrigation water management. It is apparent from these outputs that, under RCPs 4.5, 6.0 and 8.5 scenarios, annual rainfall is projected to increase by 5.6%, 3.3% and 8.7% during 2020s, 2050s and 2080s, respectively. However, RCP6.0 scenario shows a decrease in annual rainfall by 10.6%, 6.8% and 10.5% during 2020s, 2050s and 2080s, respectively.

3.1.2. Reference evapotranspiration

Fig. 8 illustrates an example of mean monthly reference evapotranspiration, ET_o, for January–December of 2017 that was projected by using a single climate model (CCSM4) under RCP4.5 scenario. The overall projected annual ET_o is 1410.2 mm, which is consistent with the expected observed ET_o values from the scheme area. All GCMs predict increase in future ET_o under RCP4.5 scenario with respect to the baseline period. The largest annual mean change in ET_o (2.9%) was obtained with CSIRO model and the lowest (0.4%) was with HadGEM2-CC model. The largest mean monthly ET_o was obtained for the dry season (March–August), with the highest value obtained for July and the lowest for November with all models.

Table 4
Projected changes of average monthly rainfall (%) in the study area for the periods 2010–2039, 2040–2069 and 2070–2099 relative to the baseline period of 1976–2005 under RCP 4.5, 6.0 and 8.5 scenarios.

Scenarios	Jan	Feb	Mar	Apr	May	Jun	Jul	Aug	Sep	Oct	Nov	Dec
RCP4.5												
2020s	16.7	13.2	18.3	6.8	6.3	–3.7	11.4	14.1	7.5	14.6	–10.3	–8.0
2050s	4.6	0.6	1.2	2.2	4.4	–2.9	2.9	10.4	7.8	17.3	3.6	–1.6
2080s	12.6	2.9	0.0	16.6	12.4	14.7	13.0	10.4	2.8	33.7	11.9	3.2
RCP6.0												
2020s	–29.2	–24.8	–23.4	–9.9	4.5	–3.4	–7.4	–10.1	–13.2	–9.3	–18.1	–18.5
2050s	–13.2	–19.5	–23.9	–4.7	–6.6	–3.4	9.1	4.9	–9.5	–5.1	–17.6	–15.8
2080s	–35.6	–26.4	–32.6	–14.9	2.0	–9.4	11.3	–2.5	–18.8	–5.4	–12.9	–16.6
RCP8.5												
2020s	6.7	6.1	8.3	10.1	0.8	–4.9	15.7	11.3	3.9	15.3	3.7	–0.4
2050s	0.3	–4.0	–5.6	5.2	9.8	4.6	8.6	11.0	9.5	7.8	11.9	–0.4
2080s	–8.3	–21.9	–31.0	–0.5	8.5	3.7	5.2	2.6	3.0	20.1	13.3	–6.8

3.1.3. Water demand projection

Irrigation requirements vary with the emission scenarios (RCPs 4.5, 6.0 and 8.5) and that high irrigation requirement is obtained for March–April where all irrigation service areas are fully planted. The model outputs also reveal that the main (wet) season (July–December) has no irrigation requirements due to heavy rainfall during that period.

3.2. Modeling hydro-climatic parameters under climate change impacts

3.2.1. Effective rainfall

Changes in effective rainfall differ considerably with the GCMs and RCP scenarios with no general trend (Table 5 and Fig. 9). The effective rainfall is projected to increase during off season from the baseline value of 386 mm by 3.4%, 0.8% and 7.6% for 2020s, 2050s and 2080s, respectively under RCP4.5; the percentage values in parenthesis are for RCP8.5. There is also a noticeable decrease of the effective rainfall (7.6%) in the late century under RCP8.5. A similar nature of variation is observed in the main season with the exception of RCP6.0 scenario. Significant decrease in rainfall is observed with the CSIRO and HadGEM2-ES models, while MPI-ESM-LR and CANESM2 models predicted marked increase in future effective rainfall. The change in rainfall is generally not defined by the characteristics of a given model, but it depends largely on the GCM's physical parameterizations (Chung and Nkomozepi, 2012). The prediction of effective rainfall is therefore a major source of uncertainty in impact assessments. Despite their variations, most GCMs predicted an increase in effective rainfall for all future scenarios under investigation. This information will help understanding water management in rice irrigation in the future.

3.2.2. Reference evapotranspiration

The annual mean maximum and minimum temperatures continuously increase in the 2020s, 2050s and 2080s over the baseline period for the three RCP scenarios (Table 6). There is a general consensus in all GCM models with respect to temperature increase in the future under all three emission scenarios. This implies that the scheme area under study is expected to be warmer in the future, especially during the off (dry) season months. This predicted future change is consistent with the IPCC findings for south-east Asia region (Stocker,

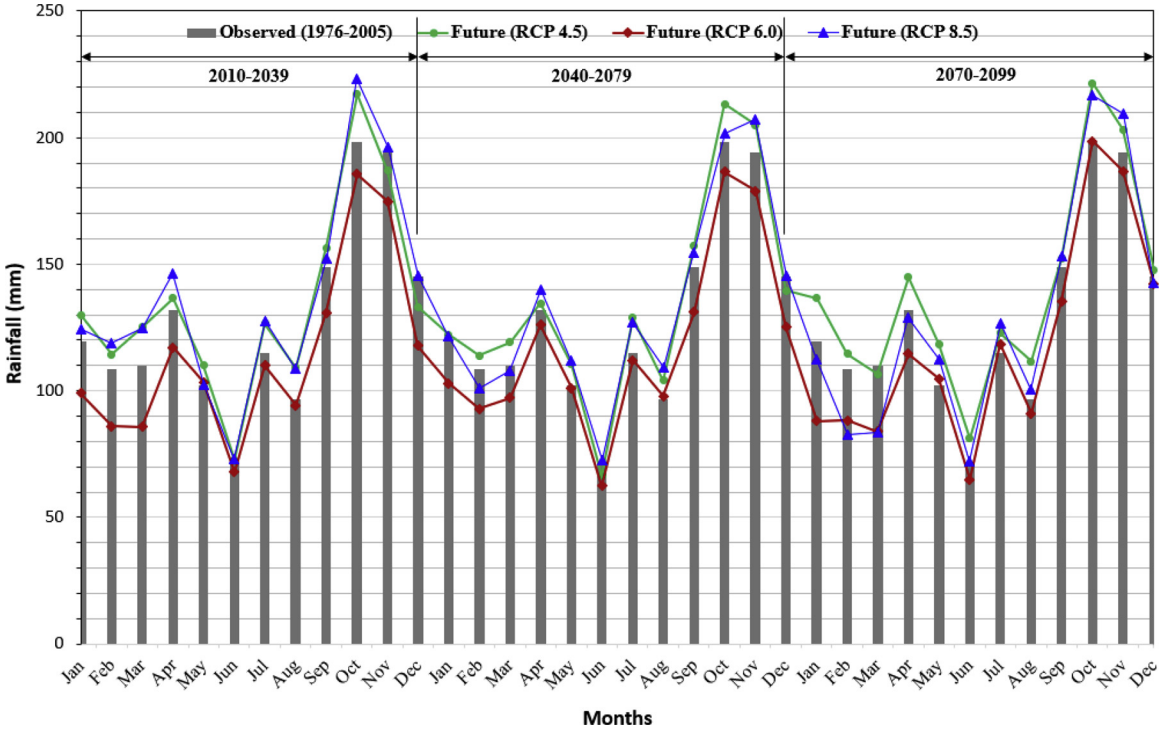

Fig. 7. Projected mean monthly rainfall from multi-models for three RCP scenarios (RCPs 4.5, 6.0 and 8.5) for three future periods of 2010–2039, 2040–2069 and 2070–2099 relative to the baseline period of 1976–2005.

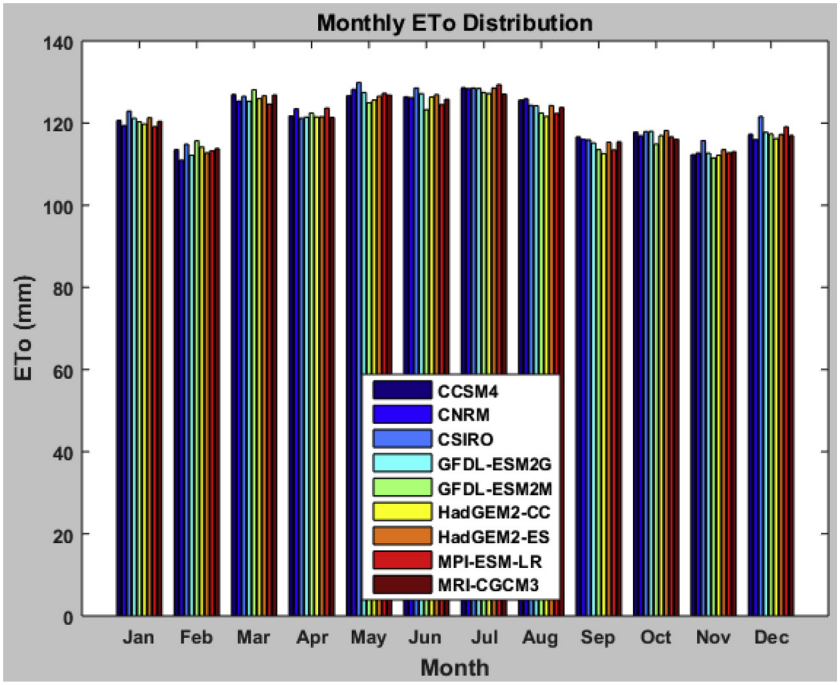

Fig. 8. Mean monthly ET_o for individual GCM models for 2050s period under RCP4.5 scenario.

2014; Solomon et al., 2007). Table 6 also presents annual changes in reference evapotranspiration, ET_o, for the three future periods under the three RCP scenarios. Under the three RCPs, ET_o increases in the scheme area by 1.6–3.7%, 0.8–4.7% and 1.6–9.1% during 2010–2039, 2040–2069 and 2070–2099 periods, respectively with respect to the baseline period of 1976–2005. The highest ET_o is 1549.8 mm under RCP 8.5 during 2080s and the lowest ET_o is 1431.6 mm under RCP6.0 during 2020s. Similar to temperature change, there is also consensus in the GCM-projected annual changes in ET_o under all scenarios throughout the future periods, with all models projecting future increase in ET_o as provided in Table 7. Significant increase in monthly ET_o is prominent during the dry season months (March–July) (Fig. 10). The highest increase is 14.2% under RCP 8.5 (most severe scenario) during the 2080s and the lowest increase is 0.2% under RCP 6.0 in the near future (2020s). The analysis unequivocally reveals that the projected increase in temperature has a direct impact on ET_o and, consequently, will have the effect on crop-water demand. The projected increase in the annual ET_o (Fig. 11) under the three RCP scenarios for the three future periods clearly demonstrates that irrigation requirements are expected to increase in the future. Therefore, climate-smart appropriate adaptation strategies will be crucial towards meeting crop-water demand under future climatic conditions.

Based on the projection, future monthly changes in temperature for the three future periods under the three RCP scenarios with respect to baseline period are expected to increase. In RCP8.5 scenario, significant monthly increase in temperature is predicted, with maximum increase between 3.5 °C and 3.7 °C. More warming is estimated during the off season in the irrigation scheme compared to the main season. The anticipated irrigation demands of the rice crop are examined for the future emission scenarios by accounting for the changes in rainfall and reference evapotranspiration. Fig. 12, based on the GCM outputs, demonstrates that more water will be needed in the future except in October and November. The predicted trends of warming due to increase in temperature are expected to cause increase in reference evapotranspiration in the future periods.

3.2.3. Crop evapotranspiration

Paddy crop evapotranspiration (ET_c) was computed by using Penman-Monteith model (Eq. (5)) based on the time-varying crop coefficient and reference evapotranspiration, ET_o. The seasonal crop evapotranspiration increases in the future periods over the baseline period following different trends for the three RCP scenarios and future periods (Table 8).

On average, ET_c for the off (dry) season varies from 1008 to

Table 5
Projected annual changes in effective rainfall (%) by GCMs under RCP 4.5, 6.0 and 8.5 scenarios for the periods 2010–2039, 2040–2069 and 2070–2099 relative to the baseline period of 1976–2005.

GCMs	RCP4.5			RCP6.0			RCP8.5		
	2020s	2050s	2080s	2020s	2050s	2080s	2020s	2050s	2080s
CANESM2	–	–	–	–	–	–	16.4	27.7	37.9
CCSM4	–1.0	3.9	4.0	–6.5	–3.0	0.6	–2.3	5.5	–3.7
CNRM	–6.6	–1.0	–4.5	–	–	–	–1.9	–7.1	0.0
CSIRO	–1.9	1.3	8.1	–4.7	–10.0	–7.1	0.3	–33.5	–72.2
GFDL-ESM2G	3.4	6.1	3.6	4.7	6.6	8.1	1.2	15.0	0.0
GFDL-ESM2M	5.6	2.9	6.5	7.2	14.5	14.2	12.0	5.1	9.3
HadGEM2-CC	13.8	–5.1	5.5	–	–	–	4.1	–1.5	0.1
HadGEM2-ES	2.0	–9.4	–0.7	–55.3	–55.5	–62.3	–0.8	–8.4	–8.2
MPI-ESM-LR	34.1	28.7	43.6	–	–	–	44.9	34.7	27.3
MRI-CGCM3	2.7	–2.9	10.1	–5.4	–0.2	–6.1	–3.2	3.9	–5.1

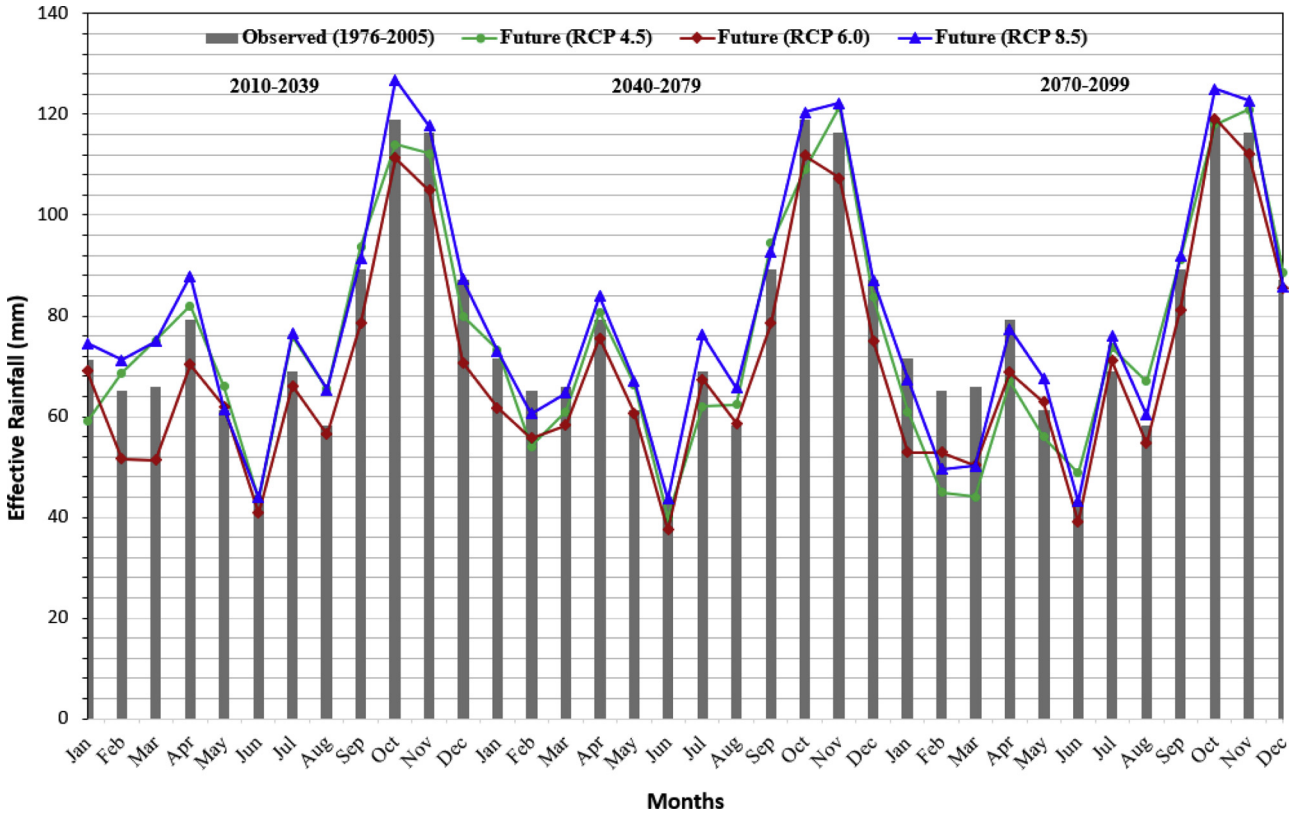

Fig. 9. Projected mean monthly effective rainfall by using multi-models for RCP 4.5, 6.0 and 8.5 scenarios for 2010–2039, 2040–2069 and 2070–2099 periods with respect to the baseline period of 1976–2005.

Table 6
Annual changes in future maximum (T_{max}) and minimum (T_{min}) temperatures and reference evapotranspiration (ET_o) under RCP4.5, RCP6.0 and RCP8.5 scenarios.

Periods	Annual changes in temperature under RCP scenario		
	RCP4.5	RCP6.0	RCP8.5
T_{max} (°C)			
2020s	0.7	0.5	0.8
2050s	1.3	1.1	1.9
2080s	1.6	1.9	3.3
T_{min} (°C)			
2020s	0.7	0.6	0.9
2050s	1.4	1.2	2.0
2080s	1.4	1.2	2.0
ET_o (%)			
2020s	1.6	0.8	1.6
2050s	3.2	2.3	4.8
2080s	3.7	4.7	9.1

1021 mm (1.1–2.5%) under RCP 4.5, 1003 to 1029 mm (0.7–3.3%) under RCP 6.0 and 1009 to 1058 mm (1.2–6.1) under RCP 8.5 scenarios. Similarly, the variation is from 948 to 958 mm (0.6–1.7%) under RCP 4.5, 945 to 961 mm (0.2–2.0%) under RCP 6.0 and 947 to 981 mm (0.5–4.1%) under RCP 8.5 during the main season. The highest ET_c for the worst case scenario (RCP 8.5) is estimated to be 8.5 mm day^{-1} (March–April) and 2.6 mm day^{-1} (June–July) during the off season. The lowest ET_c is 7.3 mm day^{-1} (September–October) and 2.3 mm day^{-1} (December–January) during the main season. As expected, ET_c is found higher in the dry season than in the wet season due to future increase in temperature and subsequent increase in ET_o in the dry season.

3.2.4. Irrigation water requirements

Irrigation requirements are higher in the off season compared to the main season. For the off season, the mean irrigation water requirement is projected to increase up to 0.1% (613 mm) under RCP 4.5, 13.7% (694 mm) under RCP 6.0 and 10.5% (675 mm) under RCP 8.5 for 2080s period with respect to baseline period (Table 9). During the main season, irrigation water requirements are projected to decrease in all three future periods and RCP 4.5 and RCP 8.5 scenarios. The projected decrease in irrigation water requirement for 2020s, 2050s and 2080s is 5.4% (382 mm), 3.8% (388 mm) and 2.9% (392 mm), respectively under RCP 4.5, and 6.8% (376 mm), l 3.2% (390 mm) and –1.7% (410 mm; increase during 2080s), respectively under RCP 8.5. The main reason for the decrease in irrigation water requirement is attributed to significant contribution from effective rainfall. However, the high–-medium RCP6.0 scenario exhibits the highest increase in irrigation water requirement in all future periods and seasons. This would be possibly due to unavailability of data for this scenario at the archives of some GCMs (CanESM2, CNRM-CM5, HadGEM2-CC and MPI-ESM-LR). The RCP 6.0 scenario should, therefore, be used with great caution in future application of the CSDSS-RIMIS tool.

February to May of the off season will require more irrigation water in the 2080s under RCP 8.5 scenario, with a maximum requirement of 29.4% in March (Fig. 13). The average irrigation requirement would be the highest (5.2 mm day^{-1}) during March–April and lowest (1.9 mm day^{-1}) during May–June. The first future period (2020s) does not show much increase in irrigation water demand under RCP 4.5 and RCP 8.5 scenarios. In the same manner, the main season will be dominated by high rainfall events, which will lead to less irrigation requirements, especially in November and December. It is revealed that effective rainfall in the study area starts exceeding the irrigation requirements in October and continues up to December/January.

In the future, irrigation water requirements in the scheme will vary significantly over the months during the off season, and the increase in effective rainfall during the main season will compensate the high water demand of the off season. Consequently, no irrigation will be

Table 7
Projected annual changes in ET_o (%) by different GCMs under RCP 4.5, RCP 6.0 and RCP 8.5 scenarios for three future periods with respect to baseline period.

GCMs	RCP4.5			RCP6.0			RCP8.5		
	2020s	2050s	2080s	2020s	2050s	2080s	2020s	2050s	2080s
CANESM2	–	–	–	–	–	–	3.6	8.2	13.3
CCSM4	1.7	3.7	4.7	2.0	2.9	6.1	2.0	5.4	10.7
CNRM	1.7	2.8	3.5	–	–	–	1.4	3.8	5.6
CSIRO	3.0	4.0	4.6	1.9	3.3	4.7	1.0	4.0	7.4
GFDL-ESM2G	1.7	3.0	3.2	1.2	2.3	3.5	2.0	3.8	6.6
GFDL-ESM2M	1.3	2.1	2.5	0.9	1.0	3.0	0.9	3.1	5.3
HadGEM2-CC	0.4	3.3	2.8	–	–	–	0.8	5.7	11.7
HadGEM2-ES	1.7	3.4	4.9	1.8	3.6	6.3	2.1	5.4	12.9
MPI-ESM-LR	1.0	3.4	2.8	–	–	–	0.4	4.4	9.9
MRI-CGCM3	1.5	2.7	4.0	–3.1	0.3	4.2	1.6	4.3	8.1

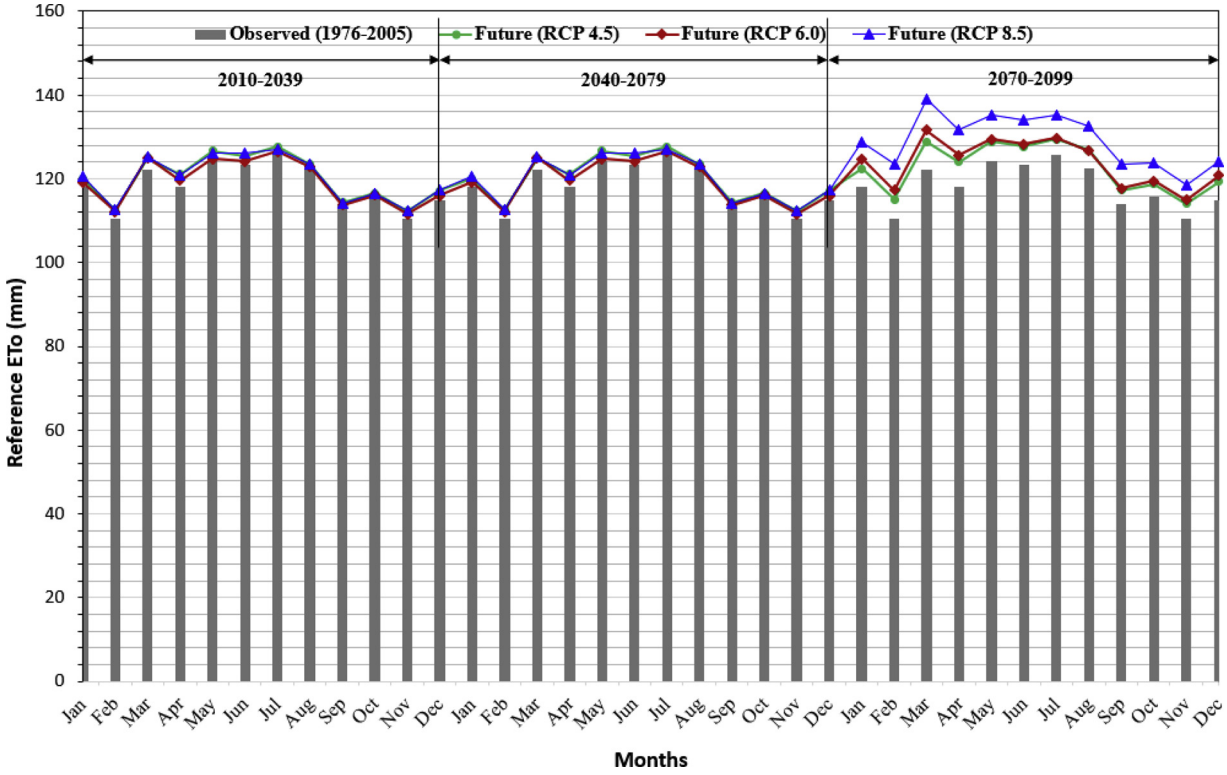

Fig. 10. Projected mean monthly reference evapotranspiration (ET_o) obtained from multi-models under RCP4.5, RCP6.0 and RCP8.5 scenarios for three future periods with respect to baseline period.

required for some months (e.g., November and December). This result is partially supported by the findings of Tukimat et al. (2017), who also revealed that climate change will not affect water abundance in the south-east Asian countries since water demand will reduce due to increase in rainfall. However, the major challenge will be to manage the monthly variability of irrigation water demand in the command area, failure to which would lead the irrigation system to much more uncertainty since the project is a run-of-the-river irrigation scheme with no storage reservoir.

4. Conclusions

A user-friendly Climate-Smart Decision Support System for Rice Irrigation Management Information System, CSDSS-RIMIS, was developed and tested successfully for simulating climate scenarios to enhance planning and management of irrigation water under future climate forcing for a large-scale irrigation scheme (Tanjung Karang Rice Irrigation Project) in Malaysia. The outputs generated by the CSDSS-RIMIS tool can be obtained through individual GCMs and/or multi-models (ensemble) projection. The outputs of the model reveal that the future challenge for efficacious irrigation in the Tanjung Karang Project will be to properly manage monthly variability in water demand that could lead to uncertainty in water supply since the project is a run-of-the-river irrigation scheme with no storage reservoir. The predicted change in irrigation water demand at the scheme is a function of changing patterns of rainfall and reference crop evapotranspiration. The CSDSS-RIMIS tool can be utilized as a guide for managing water resources under climate change scenario. It will promote appropriate adaptation and mitigation strategies like construction of storage reservoir for rainwater harvesting that can lead to sustainable water use at farm level under climate forcing. The advantage of the tool is the quick simulation of a very comprehensive information that allows water managers to make fast-decision for paddy field water management. The easy-to-use tool can also make climate change discussions more practical to water users who may not be familiar with such forums. Although the tool has been customized for local application in a tropical rice cultivation area, it can be extended to other locations by taking into account historical station data, GCMs and data of the

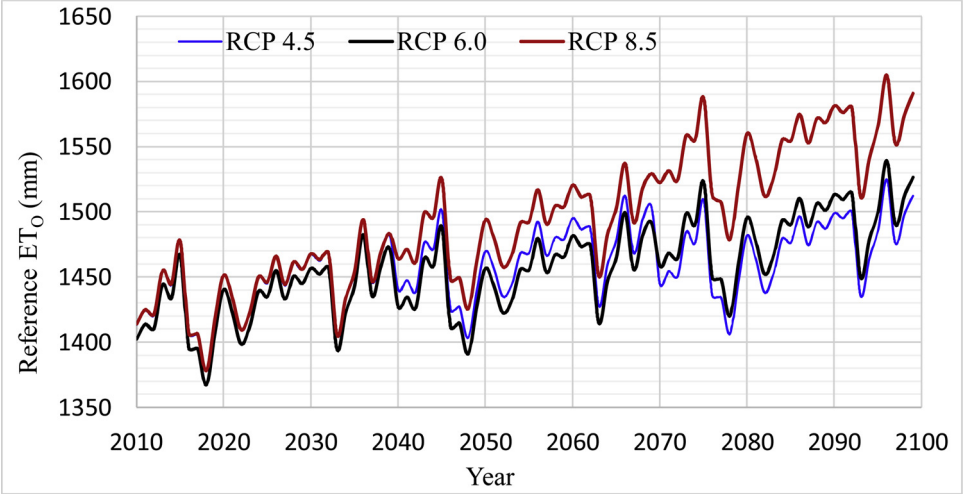

Fig. 11. Projected annual reference evapotranspiration (ET_o) obtained from multi-models under RCP4.5, RCP6.0 and RCP8.5 scenarios for three future periods.

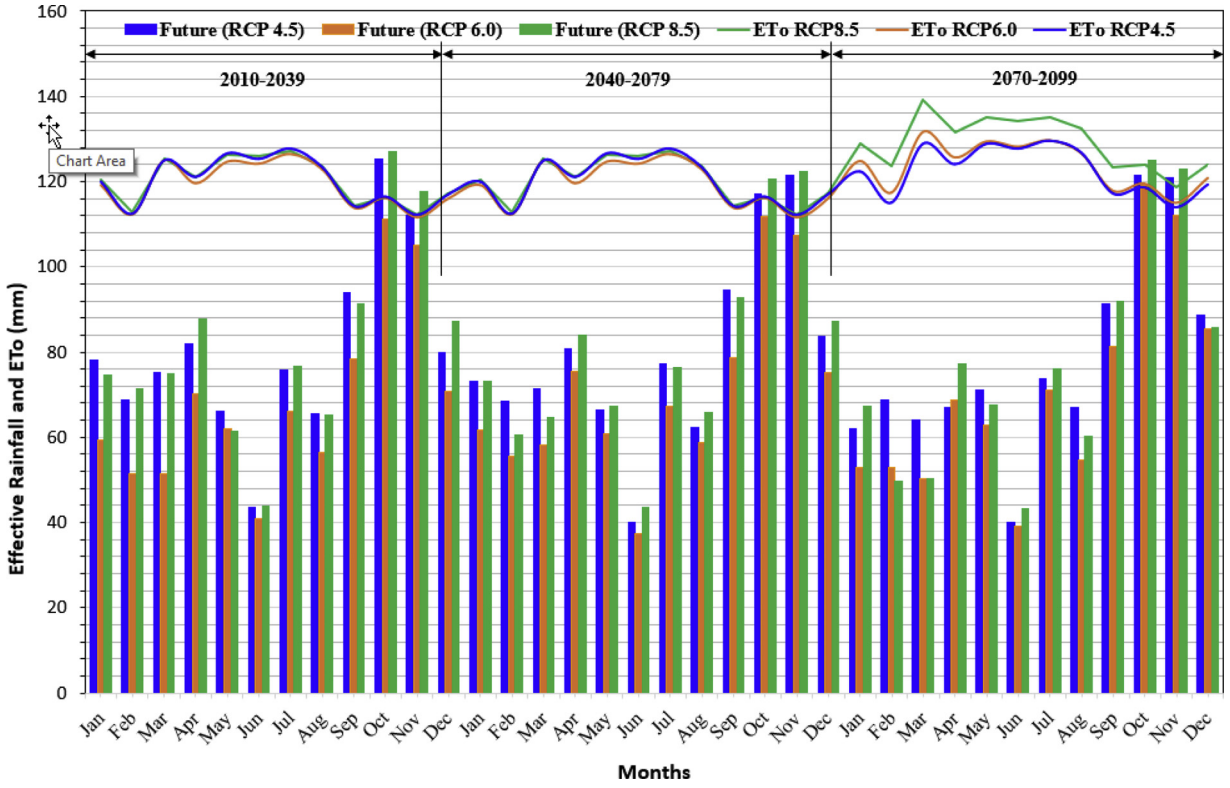

Fig. 12. Projected monthly effective rainfall and reference evapotranspiration (ET_o) using multi-models under RCP 4.5, RCP 6.0 and RCP 8.5 scenarios for three future periods.

Table 8
Annual changes in future crop evapotranspiration (ET_c %) under RCP 4.5, 6.0 and 8.5 scenarios for three future periods.

Periods	Annual changes in ET_c under RCP scenario		
	RCP4.5	RCP6.0	RCP8.5
Off season			
2020s	1.1	0.7	1.2
2050s	2.3	1.5	3.3
2080s	2.5	3.3	6.1
Main season			
2020s	0.6	0.2	0.5
2050s	1.3	1.0	2.0
2080s	1.7	2.0	4.1

Table 9
Annual changes in future irrigation water requirements (%) under RCP4.5, 6.0 and 8.5 scenarios for three future periods.

Periods	Annual changes in irrigation water requirements under RCP scenario		
	RCP4.5	RCP6.0	RCP8.5
Off-season			
2020s	–1.8	9.4	2.5
2050s	0.1	10.8	5.9
2080s	0.4	13.7	10.5
Main season			
2020s	–5.4	9.4	–6.8
2050s	–3.8	11.1	–3.2
2080s	–2.9	13.5	1.7

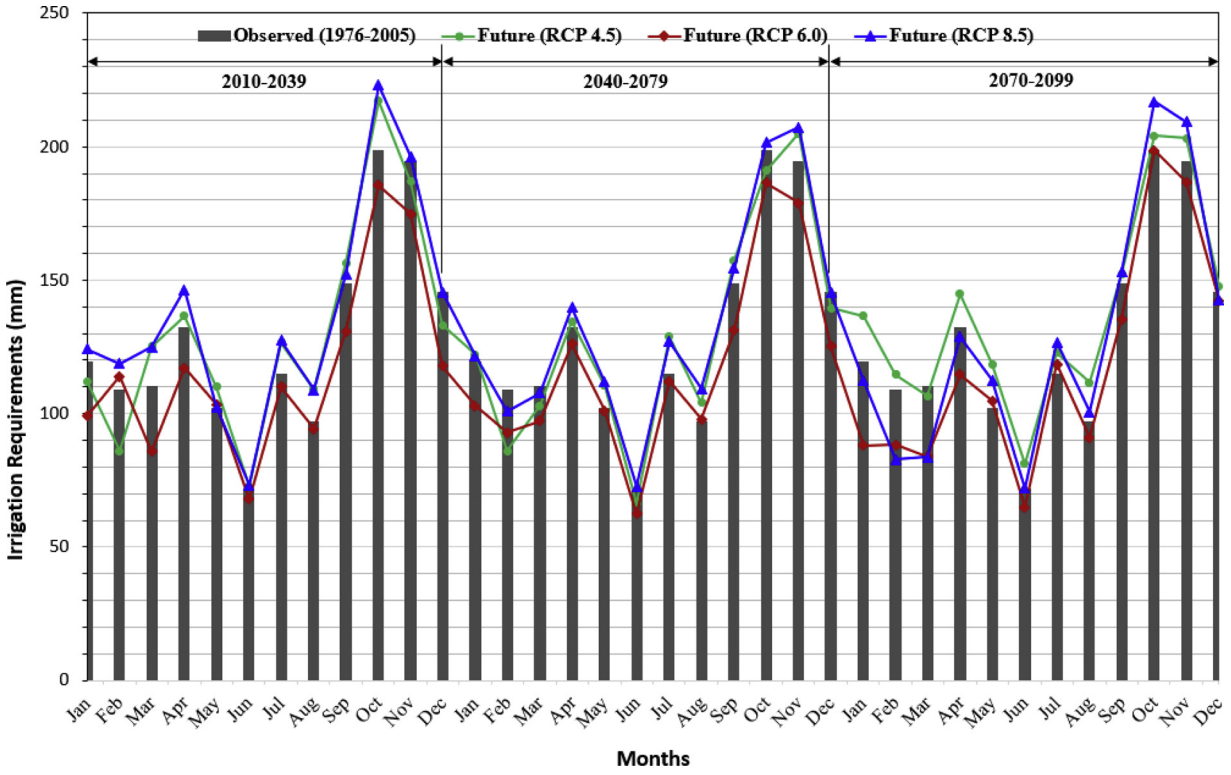

Fig. 13. Projected mean monthly irrigation water requirements using multi-models under RCP 4.5, 6.0 and 8.5 scenarios for three future periods with respect to the baseline period.

locations. In spite of these advantages, there are some limitations of the CSDSS-RIMIS tool. In this study, a popular downscaling approach, using change factors, was used that has limitations compared to other approaches. Further studies may adopt more sophisticated approaches, which will allow more detailed analysis of climate change impacts. Upgrading the GCMs with missing outputs under RCP 6.0 scenario and addition of the lowest scenario (RCP 2.5), which was not included in the current study, are needed. Future studies should include estimation of demand-based flows in the tertiary networks, including recommended irrigation supply, actual irrigation supply, volume of water, etc. These parameters have not been included in the current study, but would be important in managing water allocations.

Conflict of interest

The authors declare that there is no conflict of interest.

Acknowledgements

This research was supported by the Universiti Putra Malaysia under Putra Grants (no. 9592000, 9406300 and 9446200). The authors are grateful to the staff of the Department of Irrigation and Drainage, Department of Agriculture and National Hydraulic Research Institute of Malaysia for providing hydro-meteorological data for the study. They also acknowledge the International Modeling Groups for providing their data and Program for Climate Model Diagnosis and Inter-comparison. Sincere appreciation is also extended to the reviewers for their valuable critics and suggestions for improving the manuscript.

References

Acharjee, T.K., Fulco, L., van Halsema, G., Hellegers, P., Supit, I., 2017. Future changes in water requirements of Boro rice in the face of climate change in North-West Bangladesh. Agric. Water Manage. 194, 172–183.

Allen, R.G., Pereira, L.S., Raes, D., Smith, M., 1998. Crop Evapotranspiration-Guidelines for Computing Crop Water Requirements – FAO Irrigation and Drainage Paper 56, vol. 300. FAO, Rome, pp. 6541.

Chan, C., Cheong, A., 2001. Seasonal weather effects on crop evapotranspiration and rice yield. J. Trop. Agric. Food Sci. 29, 77–92.

Chen, J., Brissette, F.P., Leconte, R., 2011. Uncertainty of downscaling method in quantifying the impact of climate change on hydrology. J. Hydrol. (Amst.) 401, 190–202.

Chung, S.O., Nkomozepi, T., 2012. Uncertainty of paddy irrigation requirement estimated from climate change projections in the Geumho river basin, Korea. Paddy Water Environ. 10 (3), 175–185.

de Silva, C.S., Weatherhead, E.K., Knox, J.W., Rodriguez-Diaz, J.A., 2007. Predicting the impacts of climate change – a case study on paddy irrigation water requirements in Sri Lanka. Agric. Water Manage. 93 (1–2), 19–29.

De Wrachien, D., 2003. Paddy and Water environment: facilitation information exchange and identifying future R & D needs. Paddy Water Environ. 1 (1), 3–5.

Deni, S.M., Suhaila, J., Zin, W.Z.W., Jemain, A.A., 2010. Spatial trends of dry spells over Peninsular Malaysia during monsoon seasons. Theor. Appl. Climatol. 99 (3–4), 357–371.

Department of Irrigation and Drainage (DID), Japan International Cooperation Agency (JICA), 1998. The Study on Modernization of Irrigation Water Management System in the Granary Areas of Peninsular Malaysia, Nippon Koei, Kuala Lumpur, Malaysia.

Diaz, J.R., Weatherhead, E.K., Knox, J.W., Camacho, E., 2007. Climate change impacts on irrigation water requirements in the Guadalquivir river basin in Spain. Region. Environ. Change 7 (3), 149–159.

Diaz-Nieto, J., Wilby, R.L., 2005. A comparison of statistical downscaling and climate change factor methods: impacts on low flows in the River Thames, United Kingdom. Clim. Change 69, 245–268.

Doll, P., 2002. Impact of climate change and variability on irrigation requirements: a global perspective. Clim. Chang. 54, 269–293.

Elgaali, E., Garcia, L.A., Ojima, D.S., 2007. High resolution modeling of the regional impacts of climate change on irrigation water demand. Clim. Change 84, 441–461.

FAO, 2013. Climate-smart Agriculture: Policies, Practices and Financing for Food Security, Adaptation and Mitigation. Rome.

Fischer, G., Tubiello, F.N., Van Velthuizen, H., Wiberg, D.A., 2007. Climate change impacts on irrigation water requirements: effects of mitigation, 1990–2080. Technol. Forecast. Social Change 74 (7), 1083–1107.

Frederick, K.D., Major, D.C., 1997. Climate change and water resources. Clim. Change 37, 7–23.

Hargreaves, G.H., Samani, Z.A., 1982. Estimating potential evapotranspiration. J. Irrig. Drain. Div. 108 (3), 225–230.

International Panel for Climate Change (IPCC), 2007. Climate change 2007: the physical science basis. In: Solomon, S., Qin, D., Manning, M., Chen, Z., Marquis, M., Averyt, K.B., Tignor, M., Miller, H.L. (Eds.), Contribution of Working Group I to the Fourth Assessment Report of the Intergovernmental Panel on Climate Change. Cambridge University Press, Cambridge and New York 996 p. Available at. http://www.ipcc.ch/ipccreports/ar4-wg1.htm.

Jang, M.W., Choi, J.Y., Lee, J.J., 2007. A spatial reasoning approach to estimating paddy rice water demand in Hwanghaenam-do, North Korea. Agric. Water Manage. 89, 185–198.
Japan International Cooperation Agency (JICA), Department of Irrigation and Drainage (DID), 1998. Detailed Study of Water Resources Availability Northwest Selangor Integrated Agricultural Development Project. Final Report, vol. 1.
Kilsby, C., Jones, P., Burton, A., Ford, A., Fowler, H., Harpham, C., Wilby, R., 2007. A daily weather generator for use in climate change studies. Environ. Model. Softw. 22 (12), 1705–1719.
Kirby, J., Ahmad, M., Mainuddin, M., Palash, W., Quadir, M., Shah-Newaz, S., Hossain, M., 2015. The impact of irrigation development on regional groundwater resources in Bangladesh. Agric. Water Manage. 159, 264–276.
Kirby, J., Mainuddin, M., Mpelasoka, F., Ahmad, M., Palash, W., Quadir, M., Shah-Newaz, S., Hossain, M., 2016. The impact of climate change on regional water balances in Bangladesh. Clim. Change 135, 481–491.
Knox, J.W., Díaz, J.R., Nixon, D., Mkhwanazi, M., 2010. A preliminary assessment of climate change impacts on sugarcane in Swaziland. Agric. Syst. 103 (2), 63–72.
Lee, T.S., Haque, M.A., Najim, M., 2005. Scheduling the cropping calendar in wet-seeded rice schemes in Malaysia. Agric. Water Manage. 71 (1), 71–84.
McKague, K., Rudra, R., Ogilvie, J., 2003. CLIMGEN – a convenient weather generator tool for Canadian climate stations. Meeting of the CSAE/SCGR Canadian Society for Engineering in Agricultural Food and Biological Systems. http://www.sipeaa.it/tools/ClimGen/CSAE03-118.pdf.
Mojid, M., Rannu, R., Karim, N., 2015. Climate change impacts on reference crop evapotranspiration in north-west hydrological region of Bangladesh. Int. J. Climatol. 35, 4041–4046.
Nicks, A.D., Lane, L.J., Gander, G.A., 1995. Weather Generator. USDA-Water Erosion prediction Project: Hillslope Profile and Watershed Model Documentation. USDA-ARS National Soil Erosion Research Laboratory, pp. 1–22 (chapter 2).
Ouyang, F., Zhu, Y., Fu, G., Lü, H., Zhang, A., Yu, Z., Chen, X., 2015. Impacts of climate change under CMIP5 RCP scenarios on streamflow in the Huangnizhuang catchment. Stoch. Environ. Res. Risk Assess. 29, 1781–1795.
Rehana, S., Mojumdar, P.P., 2012. Climate change induced risk in water quality control problems. J. Hydrol. (Amst.) 444–445, 63–77.
Risbey, J.S., Entekhabi, D., 1996. Observed Sacramento Basin stream flow response to precipitation and temperature changes and its relevance to climate impact studies. J. Hydrol. (Amst.) 184 (3–4), 209–223.
Rowshon, M., Mojid, M., Amin, M.S.M., Azwan, M., Yazid, A., 2014. Improving irrigation water delivery performance of a large-scale rice irrigation scheme. J. Iirrig. Drain. Eng. 140 (8) p. 04014027.
Schlenker, W., Hanemann, W.M., Fisher, A.C., 2007. Water availability, degree days and the potential impact of climate change on irrigated agriculture in California. Clim. Change 81, 19–38.
Semenov, M.A., Barrow, E.M., Lars-Wg, A., 2002. A Stochastic Weather Generator for Use in Climate Impact Studies. User's Manual, Version, 3.
Shahid, S., 2011. Impact of climate change on irrigation water demand of dry season Boro rice in north-west Bangladesh. Clim. Change 105, 433–453.
Sharpley, A.N., 1990. EPIC-Erosion/productivity Impact Calculator: 1. Model Documentation. Technical Bulletin 1768. US Department of Agriculture 235p.
Solomon, S., Qin, D., Manning, M., Averyt, K., Marquis, M., 2007. Climate Change 2007-the Physical Science Basis: Working Group I Contribution to the Fourth Assessment Report of the IPCC, vol. 4 Cambridge University Press.
Stocker, T., 2014. Climate Change 2013: The Physical Science Basis: Working Group I, Contribution to the Fifth Assessment Report of the Intergovernmental Panel on Climate Change. Cambridge University Press, Cambridge, UK.
Tukimat, N.N.A., Harun, S., Shahid, S., 2017. Modeling irrigation water demand in a tropical paddy cultivated area in the context of climate change. J. Water Resour. Plan. Manage. 143 (7) p. 05017003.
Wang, Z.K., Wu, P.T., Zhao, X.N., Cao, X.C., Gao, Y., 2014. GANN models for reference evapotranspiration estimation developed with weather data from different climatic regions. Theor. Appl. Climatol. 116 (3–4), 481–489.
Wilby, R.L., Harris, I., 2006. A framework for assessing uncertainties in climate change impacts: low-flow scenarios for the River Thames, UK. Water Resour. Res. 42 (2), W02419.
Wilby, R.L., Dawson, C.W., Barrow, E.M., 2002. SDSM—a decision support tool for the assessment of regional climate change impacts. Environ. Model. Softw. 17 (2), 145–157.
Wong, C., Venneker, R., Uhlenbrook, S., Jamil, A., Zhou, Y., 2009. Variability of rainfall in Peninsular Malaysia. Hydrol. Earth Syst. Sci. Discuss. 6, 5471–5503.
Wong, C., Venneker, R., Jamil, A., Uhlenbrook, S., 2011. Development of a gridded daily hydro-meteorological data set for Peninsular Malaysia. Hydrol. Process. 25, 1009–1020.
Yano, T., Aydin, M., Haraguchi, T., 2007. Impact of climate change on irrigation demand and crop growth in a Mediterranean environment of Turkey. Sensors 7, 2297–2315.
Ye, Q., Yang, X., Dai, S., Chen, G., Li, Y., Zhang, C., 2015. Effects of climate change on suitable rice cropping areas, cropping systems and crop water requirements in southern China. Agric. Water Manage. 159, 35–44.
Yoo, S.H., Choi, J.Y., Nam, W.H., Hong, E., 2012. Analysis of design water requirement of paddy rice using frequency analysis affected by climate change in South Korea. Agric. Water Manage. 112, 33–42.
Yoo, S.H., Choi, J.Y., Lee, S.H., Gyeong, O.Y., Yun, D.K., 2013. Climate change impacts on water storage requirements of an agricultural reservoir considering changes in land use and rice growing season in Korea. Agric. Water Manage. 117, 43–54.
Zin, W.Z.W., Jamaludin, S., Deni, S.M., Jemain, A.A., 2010. Recent changes in extreme rainfall events in Peninsular Malaysia: 1971–2005. Theor. Appl. Climatol. 99 (3–4), 303–314.